Heat Mass Transfer
DOI 10.1007/s00231-015-1652-x

ORIGINAL

Study on heat transfer coefficients during cooling of PET bottles for food beverages

Antonio Liga[1] · Salvatore Montesanto[1] · Gianluca A. Mannella[1] · Vincenzo La Carrubba[1] · Valerio Brucato[1] · Marco Cammalleri[2]

Received: 23 February 2015 / Accepted: 27 July 2015

Abstract The heat transfer properties of different cooling systems dealing with Poly-Ethylene-Terephthalate (PET) bottles were investigated. The heat transfer coefficient (U_g) was measured in various fluid dynamic conditions. Cooling media were either air or water. It was shown that heat transfer coefficients are strongly affected by fluid dynamics conditions, and range from 10 W/m^2 K to nearly 400 W/m^2 K. PET bottle thickness effect on U_g was shown to become relevant under faster fluid dynamics regimes.

List of symbols

A	Sample A
A_S	Bottle external area
B	Sample B
C	Constant
c_p	Specific heat
D	Bottle external diameter
g	Gravitational acceleration
Gr	Grashof Number
H	Bottle height
h_1	Heat transfer coefficient inside the bottle
h_2	Heat transfer coefficient outside the bottle
k	PET thermal conductivity
k_w	Water thermal conductivity
L	Characteristic length, volume/surface
m	Mass
Nu	Nusselt number
Pr	Prandtl number
r_1	Bottle internal radius
r_2	Bottle external radius
Q_{tot}	Global heat flux
Q_{rad}	Radiant heat flux
Q_{conv}	Convective heat flux
h_{rad}	Radiant heat transfer coefficient
$U_{conv.+cond.}$	Convective heat transfer coefficient
Ra	Rayleigh number
Re	Reynolds number
T	Temperature
T_1	Inside temperature of water
T_2	Outside temperature of cooling fluid
T_0	Initial inside temperature of water
T_g	Glass transition temperature
T_{wall}	Bottle surface temperature
T_∞	Bulk temperature of cooling fluid
θ	Dimensionless temperature
t	Time
U_g	Global heat transfer coefficient

Greek symbols

α	Thermal diffusivity
α_w	Water thermal diffusivity
α_{PET}	PET thermal diffusivity
β	Volumetric thermal expansion coefficient
δ	PET layer thickness
μ	Viscosity
ν	Kinematic viscosity (μ/ρ)
ρ	Density
τ	Characteristic time

✉ Gianluca A. Mannella
gianluca.mannella@unipa.it

[1] Department of Civil, Environmental, Aerospace and Materials Engineering (DICAM), University of Palermo, Viale delle Scienze, Ed. 8, 90128 Palermo, Italy

[2] Department of Chemical, Management, Computer and Mechanical Engineering (DICGIM), University of Palermo, Viale delle Scienze, Ed. 8, 90128 Palermo, Italy

Published online: 26 August 2015

1 Introduction

Several operations require a cooling step and, sometimes, the possibility to accurately control temperature determines their success or failure. In food, pharmaceutical and bioprocess industries, some compounds, if held above a certain temperature, may be subjected to serious deterioration issues, such as proteins or active principles denaturation, [1] compounds biodegradation [2], organoleptic properties loss [3]. High temperature steps are often needed during manufacturing operations: therefore, in this case, a fast quench final step is often mandatory. Heat transfer in solid systems, e.g. freezing of peas, beans etc. has been studied in different conditions, due to the practical relevance of the issue and the unpredictability of the nonlinear systems often encountered in food industry [4]. When operating with a liquid stream, it is very common to use heat exchangers as cooling devices. High Temperature Short Time (HTST) pasteurization allows one to maintain beverages with flavor and properties of the fresh product, without sacrificing the high safety degree of pasteurized aliments. Nevertheless, HTST methods require a sophisticated technology for temperature control [5].

Carrying out pasteurization process right before, or even after packaging, presents multiple advantages, such as preventing fluid from new contamination after the process and creating vacuum inside the container, thus slowing down product spoilage. Nevertheless, after packaging, the heat transfer is generally harder to be enhanced, owing to the geometry constraints, and it proceeds more slowly. In fruit juice canning, fluid is heated up to 80 °C by mean of heat exchangers, and then sealed inside containers. Therein, it is heated and kept at 100–105 °C for up to 10 min and then cooled down. Heat transfer is enhanced using rotary or spin action. Hot fill, a similar but more effective operation, consists in heating the processed beverage up to 95 °C for a very short time, sealing it inside containers and then directly performing the cooling, always by means of rotating devices [6].

Dynamic Irreversible Thermoporation (DIT) is a new pasteurization technique characterized by temperature increases up to 30 °C/s, with final temperatures up to 65 °C in order to create permanent holes in bacteria cellular membrane, thus causing their death [7]. If this final temperature is held for too long, containers (usually made of Poly-Ethylene-Terephthalate (PET), $T_g \approx 79$ °C) can be compromised. Moreover, additives, degradation compounds, and NIAS (Non-Intentionally Added Substances) can migrate from the container walls and dissolve in the processed food, this resulting in spoilage of organoleptic properties and risks for consumers' health [8].

From the aforementioned scenario, it is easy to understand that heat exchange around containers is particularly important in many industrial applications and its role is even more significant when heat sensitive aliments, or materials, are involved in the process. However, it is still hard to find in literature reliable data on this topic. Any different container exhibits its own characteristics and, above all, wall shape and thermal conductivity will be the most important ones. Materials and manufacturing techniques will define wall thermal conductivity (hence, for polymers: crystallinity, chains orientation etc.). Surface to volume ratio plays an important role and shape is proven to affect fluid dynamic conditions during heating and cooling of containers [9] and, in particular, of bottles in water immersion [10]. Therefore, transport properties need to be determined for the actual system considered.

In this paper, the attention was focused on the heat transfer features of two typologies of 0.5 l capacity PET bottles, currently employed in the food industry market. Because of its capacity to prevent O_2 and CO_2 permeation, PET has become a benchmark for bottling beverages, and its use is nowadays spread all over the world. The paper analyses the cooling effectiveness of an after-packaging pasteurization process on beverages contained in PET bottles, in order to assess the capabilities of the heat transfer protocols adoptable when cooling in different conditions (natural and forced convection, static and rotating bottle). The bottles used for experimental had similar shape and differ only for PET wall thickness. This means that the shape effects are similar for both samples, thus not affecting a direct comparison between results and allowing an easier study on PET thickness relevance on heat transfer. Cooling was performed both under static conditions, i.e. with motionless bottles, and dynamic conditions, i.e. by making bottle spin around its horizontal axis at 200 rpm.

Data interpretation was supported by a simplified modeling (i.e. adopting a lumped system approximation) and by heat transfer coefficient estimation via literature correlations. This approach allowed to highlight the role of each medium (fluid inside the bottle, PET layer and surrounding fluid) on global heat transfer coefficient, thus showing the limiting resistance for each case explored. Moreover, some important aspects were individuated, e.g. the onset of internal natural convection and the influence of PET thickness in distinct cases.

Although heat exchange around containers has been investigated and applied for many years, the conditions usually reported are different to those explored in our study. A lot of work has been done for measuring and correlating local Nusselt number for flow past cylinders and natural convection analysis around heated cylinders [11, 12]. Here, we tested transient situations, i.e. with the fluid inside the bottle being cooled, or arrangement with rotatory movement of bottle (which affects both internal and external convection). Within our best knowledge, no studies of these situations are available in literature.

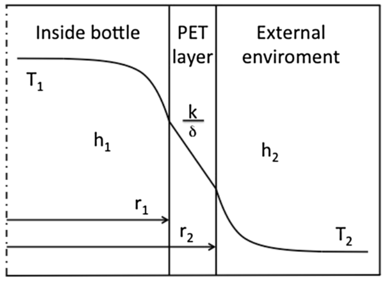

Fig. 1 Schematic section of the studied system

2 Theory and methodology

For theoretical treatment purpose, bottles were considered as cylinders of dimensions 18 × 6.6 cm (height × diameter). The global heat transfer resistance for the considered system is given by the sum of three thermal resistances in series. These are the convective resistances, for water inside the bottle (h_1) and for the outer environment (h_2), and the conductive resistance of the PET layer (See Fig. 1). This latter is a function of the layer thickness and of the thermal conductivity, and is a constant contribution for each sample type. On the contrary, internal and external fluid dynamic conditions vary with different experimental tests. Although the system presents a cylindrical symmetry, the wall thickness is about two order of magnitude smaller than bottle radius, thus the global heat transfer coefficient can be estimated assuming a planar geometry [13]:

$$U_g = \left[\frac{1}{h_1} + \frac{\delta}{k} + \frac{1}{h_2}\right]^{-1} \tag{1}$$

In the following calculations, the thermal conductivity k was fixed to 0.4 W/m K, taking the highest value from literature data. Indeed, it has been showed that orientation positively affects polymer thermal conductivity [14, 15], thus it may be speculated that the higher level of alignment among polymer chains, due to stretching during bottle blow moulding, could increase the PET thermal conductivity.

Figure 1 shows a hypothetical temperature trend: natural convection inside and outside the bottle was assumed, and planar geometry hypothesis leads to a linear tendency through the PET layer.

The heat balance on the water inside the bottle, assumed as a lumped system is:

$$mc_p\frac{dT}{dt} = -U_gA_s(T_1 - T_2) \tag{2}$$

where m is the mass of water, c_p the specific heat at constant pressure, A_s the outer bottle surface, T_1 the representative temperature for the water inside the bottle and T_2 the temperature at the bulk of cooling medium. Solving this differential equation with the boundary condition of $T_1 = T_0$ at t = 0, the function $T_1(t)$ is obtained:

$$T_1 = T_2 + (T_0 - T_2)e^{\left(-\frac{U_gA_s}{mcp}t\right)} \tag{3}$$

The lumped system approximation requires that water temperature inside the bottle can be considered uniform, i.e. when core and wall temperatures are close enough [13]. In our tests Eq. 3 was closely followed in most of cases and only calculations of U_g for static cooling in water presented a deviation from this behavior. Moreover, as shown in the Results section, natural convection occurs inside the bottle for all the conditions tested: this fact supports the assumption that temperature drop inside the bottle is confined in the boundary layer, i.e. a thin region close to the bottle surface.

A more thorough dissertation on heat transfer around the systems studied, needs to take into account heat loss by radiation. Considering that the whole heat flux is composed by both radiant and convective contributions:

$$Q_{tot} = U_gA_s(T_1 - T_2) = Q_{rad} + Q_{conv} = h_{rad}A_s(T_1 - T_2) + U_{conv+cond}A_s(T_1 - T_2) \tag{4}$$

it follows that the U_g experimentally found during our tests are always the sum of h_{rad} and $U_{conv+cond}$, i.e. the global heat transfer coefficient related to internal/external convection and conduction across PET layer. By assuming the system as a grey body with emissivity ε = 0.96, the heat lost by radiation can be estimated as:

$$Q_{rad} = \sigma\varepsilon A_s\left(T_1^4 - T_2^4\right) = \sigma\varepsilon A_s\left(T_1^2 + T_2^2\right)(T_1 + T_2) \times (T_1 - T_2) = h_{rad}A_s(T_1 - T_2) \tag{5}$$

where σ is the Stefan-Boltzmann constant, A_s is the exchange surface and h_{rad} is the equivalent heat transfer coefficient for radiation [$h_{rad} = \sigma\varepsilon\left(T_1^2 + T_2^2\right)(T_1 + T_2)$].

At time t = 0, when T_1 is 60 °C and T_2 is 20 °C, h_{rad} takes its maximum value of 6.7 W/m^2 K and drops to 0 when the system reaches equilibrium. Because of its low value, when compared to the U_g experimentally calculated, the contribution of radiant heat was coherently neglected in our dissertation.

For a better understanding of the system, some limit case studies were analyzed preliminarily. Details of this theoretical analysis are shown in "Appendix", while in the following the most important results are summarized. The theoretical heat transfer coefficient for pure diffusive heat transfer inside the bottle was calculated both mathematically and via COMSOL simulation, giving results close to 10^{-2} W/m^2 K (characteristic time = 7600 s) ("Internal heat transfer coefficient" section).

Any experimentally found U_g, higher than the one calculated for pure diffusive heat transfer, would imply that natural convection is occurring within the bottle.

To get an estimate of external heat transfer coefficients (h_2) during static cooling in air and water, and dynamic

Table 1 Empirical correlation results for h_2 in different conditions

	Air h_2 (W/m^2 K)	Water h_2 (W/m^2 K)
Horizontal position Eq. 10	5.6	985
Horizontal position Eq. 11	5.3	698
Vertical position Eq. 12	5.5	988
Vertical position Eq. 13	5.5	706
Horizontal, spinning [16]	17	

cooling in air, different empirical correlations were employed ("External heat transfer coefficient" section). Results are shown in Table 1.

Thereafter, the influence of PET layer thickness (δ) on the global heat transfer coefficient was highlighted by rearranging Eq. 3. Equation 6 shows that the time (t) necessary to reach a certain dimensionless temperature ($\theta = (T_1–T_2)/(T_0–T_2)$) approaches a linear dependence on δ when the convective heat coefficients h_1 and h_2 tend to infinite.

$$t = -\frac{mc_p}{A_s}\left(\frac{1}{h_1}+\frac{1}{h_2}+\frac{\delta}{k}\right)\ln\theta \tag{6}$$

During testing, two different typologies of bottles (0.5 L volume), both employed commercially, were used (sample A and B). Bottle A is used for still water whereas bottle B for sparkling water. Average wall thickness was evaluated as 200 µm for bottle A and 300 µm for bottle B. In all experiments, distilled water was heated up to 60 °C by means of a thermostatic bath and poured inside the bottle. Static cooling was carried out in air, water and with a downward water spray, with bottles positioned both vertically and horizontally. Dynamic cooling was realized by making a bottle rotating at 200 rpm around its axis, thanks to an electric motor. In this case, air and water spray were employed as cooling media. Bottles were clamped to the motor by the cap by using a modified spindle. Dynamic tests were conducted with bottles in horizontal position only.

In static cooling tests, four T type thermocouples (Omega, TT-T-30-SLE-100) were fastened inside the bottle (see Fig. 2a). Two of those were secured to a thin metal stick placed in correspondence with the bottle axis, one in the bottle center (T1), and the other one at about 3 cm from the cap (T2). The metal stick and thermocouples wires were fixed to a bottle cap, and easily moved from one sample to another after tests. The two remaining thermocouples were fixed near the PET wall, with a 90° offset. This configuration allowed one, during horizontal position cooling, to monitor wall temperature laterally (T3) and simultaneously in the upper side (T4). Indeed, it was shown by many authors that local heat transfer coefficient remarkably changes along the circumference of a horizontal cylinder during natural convection [16]. Holes allowing thermocouples wires passage were sealed with epoxy resin (Loctite 406). In order to collect data in real time, a I/O data acquisition device was employed (NI USB-6210, National Instruments), which allowed data recording via a LabVIEW© Virtual Instrument.

In dynamic cooling tests, only two thermocouples (one in the bottle center, the other on the PET wall) were used. As a matter of fact, when the bottle rotates, no differences in temperature at a fixed radius are expected and the two external thermocouples would reasonably measure the same temperature. The zones close to the bottle cap or bottom may have a temperature slightly lower than on the bottle axis, but owing to the good agitation of the system, those non-homogeneities are located in very small regions, thus not affecting the assumption of uniform temperature distribution. In this case, the metal stick used as a support for the central thermocouple was fixed at the bottom, being the cap clamped to the motor spindle (see Fig. 2b). Operating in horizontal position prevented the air inside the bottle from being confined in the top part of the bottle only. Data collection took place, according to a discontinuous procedure, at certain time intervals, owing to the difficulty

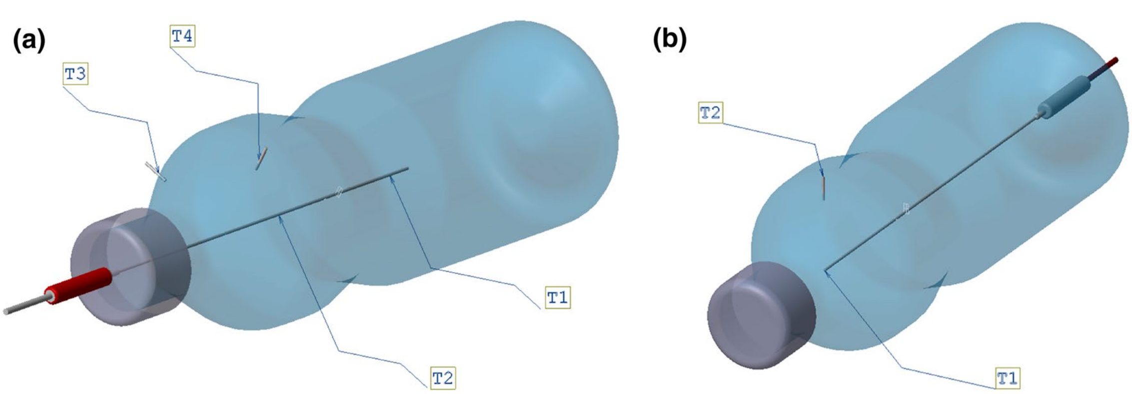

Fig. 2 Schematic of bottle with thermocouples used for measurements. **a** Static cooling. **b** Dynamic cooling

to wire a data acquisition device to a rotating bottle. For air cooling, measurement were effectuated after 2, 5, 10 and 20 min. For water spray cooling, temperature data were taken after 1, 2, 3 and 5 min.

After data collection, temperature versus time curves were plotted and bottle core temperature was fitted with Eq. 3 by using U_g (the global heat transfer coefficient) as the fitting parameter, in this way it was determined the average U_g for each cooling system analyzed. Three runs were performed for each sample type.

3 Results and discussion

3.1 Static cooling in air

In this case, experimental global heat transfer coefficients were about 10 W/m^2 K for horizontal cooling and 9 W/m^2 K for vertical cooling. These values are much higher than the one calculated for pure diffusive heat transfer inside the bottle. This fact demonstrates the presence of convection phenomena in the water inside the bottle. Therefore, convection must be present also in the other cooling cases, where external transfer is further enhanced. No differences among sample A and B were found, due to the slow transport in air (Table 1) compared to those expected for PET layer, as k/δ is about 2000 W/m^2 K for bottle A and 1330 W/m^2 K for bottle B. Thermocouples placed internally (T1 and T2) and near the surface (T3 and T4) recorded a practically identical trend (and temperature curves at bottle center are superimposed), as water convection inside the bottle is much faster than heat transport in air (see Fig. 3).

In this case, heat loss due to radiation can be relevant. Since h_{rad} ranges between 7 and 0 W/m^2 K, as a first estimate, the measured convective heat transfer coefficient can be considered close to 5 W/m^2 K, which is in good agreement with the one calculated by means of empirical correlations (Table 1).

Heat transfer by radiation was neglected in other cases, as the measured heat transfer coefficient was at least one order of magnitude higher than h_{rad}.

3.2 Static cooling in water

Global heat transfer coefficients were about one order of magnitude higher than the ones measured for the previous case. The first 30–40 s of heat exchange, in each test, were neglected, due to the rapid fluid dynamic regime variation during bottle immersion in water (see Fig. 4). Indeed, an irregular temperature profile was recorded while the regime evolved from forced convection, due to the quick immersion, to the natural convection regime typical of the system: therefore, this period was not considered helpful for the determination of a transport coefficient. For bottle A, U_g ranged around 170 W/m^2 K for horizontal cooling and 135 W/m^2 K for vertical one. For bottle B, results led to U_g of 120 and 100 W/m^2 K respectively for horizontal and vertical case.

The differences recorded among samples A and B cannot be attributed to the higher heat transfer resistance of PET in sample B only. Indeed, if writing U_g for case A and B according to Eq. 2:

$$\frac{1}{U_{gA}} = \frac{1}{h_{1A}} + \frac{1}{h_{2A}} + \frac{\delta_A}{k} \quad \text{and} \quad \frac{1}{U_{gB}} = \frac{1}{h_{1B}} + \frac{1}{h_{2B}} + \frac{\delta_B}{k} \tag{7}$$

and, assuming $h_{2A} = h_{2B}$:

$$\frac{1}{U_{gA}} - \frac{1}{U_{gB}} = \frac{1}{k}(\delta_A - \delta_B) + \left(\frac{1}{h_{1A}} - \frac{1}{h_{1B}}\right) \tag{8}$$

As the left-hand term takes values of the order of 2.5 10^{-3} m^{2}K/W and the term related to the difference in PET thickness, $\frac{1}{k}(\delta_A - \delta_B)$, is of the order of 2.5 10^{-4} m^{2}K/W, it

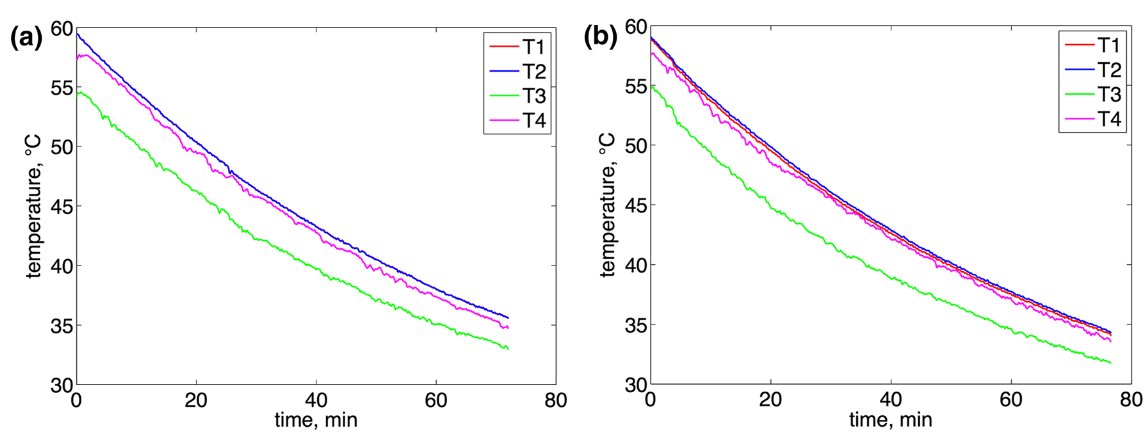

Fig. 3 Temperature measured at different locations for horizontal static cooling in air. **a** Sample A. **b** Sample B

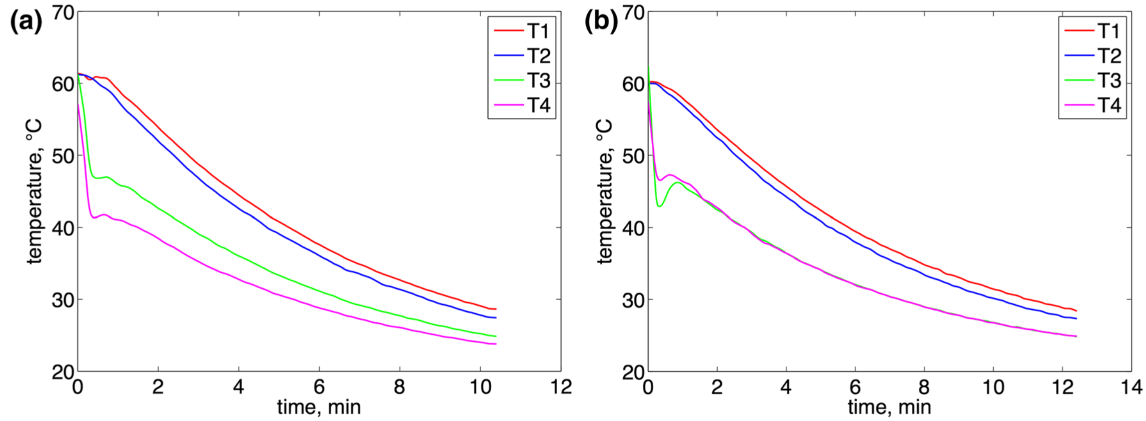

Fig. 4 Temperature measured at different locations for vertical static cooling in water. **a** Sample (a). **b** Sample (b)

Fig. 5 Illustrative representation of PET thickness influence on natural convection phenomena

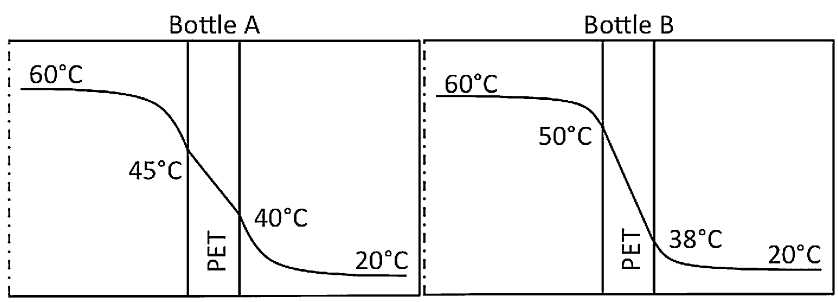

directly follows that fluid dynamics conditions inside the bottle are not the same when using different samples. In particular, the phenomenon can be explained by invoking a more intense convection in sample A. Indeed, being the temperature drop through the PET layer lower in case A than in case B, this determines higher temperature differences inside the internal and external environments, enhancing that way natural convection phenomena (illustrative example in Fig. 5).

U_g were significantly lower than h_2 determined with empirical correlations, which could mean, in this case, that internal transport and PET layer resistance play an important role in heat transfer conditions. Also, calculations showed that the different PET thickness brings the outer wall temperature from 32 °C for bottle A to 29 °C for bottle B (horizontal case), thus leading to h_2 nearly 10 % lower for the latter case.

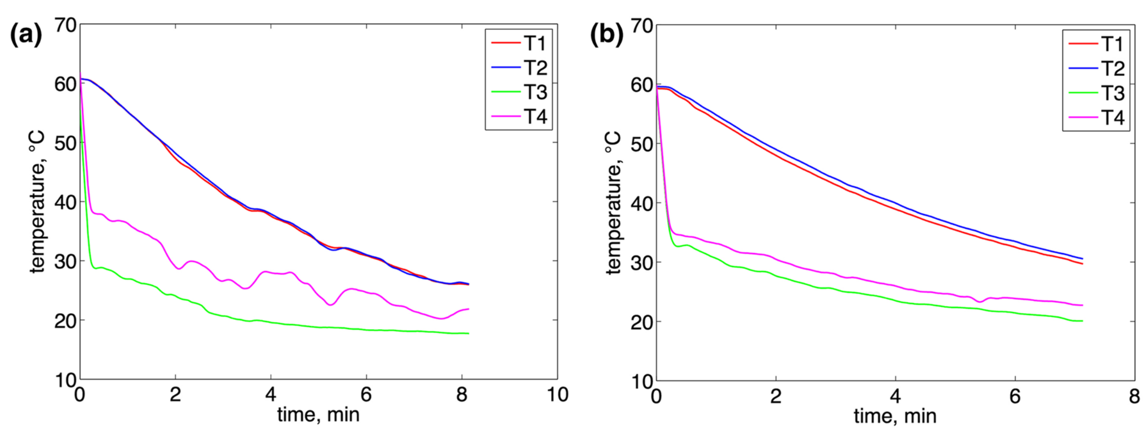

Fig. 6 Temperature measured at different locations for horizontal static cooling in water spray. **a** Sample A. **b** Sample B

3.3 Static cooling in water spray

In the horizontal case (see Fig. 6), global heat transfer coefficient was about 160 and 150 W/m^2 K for sample A and B respectively. In vertical cooling U_g were near to 130 W/m^2 K with both sample types. It must be noticed that U_g for sample A are practically the same of the ones found for previous case. On the contrary, sample B shows enhanced transport properties. Moreover, the differences found among the two sample types can be attributed, in this case, to the higher heat resistance of sample B PET layer only, as Eq. 7 gives $\frac{1}{U_{gA}} - \frac{1}{U_{gB}} \approx \frac{1}{k}(\delta_A - \delta_B)$. This led to the idea that, enhancing the external transport properties, hence increasing the temperature drop in the internal environment, the natural convection inside the bottles increases accordingly. The improvement in heat transfer coefficient, in comparison to the static cooling case, could not be noticed in sample A. As a matter of fact, the enhancement of external heat transfer did not increase the overall transfer coefficient, thus suggesting that the controlling resistance is the internal one. Therefore, it can be hypothesized that internal convection was already well developed is sample A in still water cooling case.

3.4 Dynamic cooling in air

Global heat transfer coefficient was about 15 W/m^2 K for both sample A and B. As in the case of static cooling in air, no differences were found between the samples, due to the slow external regime (see Fig. 7). Bottle rotation enhanced transport conditions, with respect to the static case, by a 50 %. Measured coefficient closely fit with the one found using Elghnam correlation (see "External heat transfer coefficient" section).

3.5 Dynamic cooling in water spray

This condition gave out the highest U_g measured in our tests. For sample A heat transfer coefficient was nearly 390 W/m^2 K, while for sample B it was about 320 W/m^2 K. As expected, fluid dynamic conditions are reasonably the same for both samples, as they are related to the rotation speed imposed by the electrical motor and not to natural convection (see Fig. 7): Eq. 8 showed that differences in U_g can be attributed to the different PET layer thickness alone.

3.6 Reliability of lumped system approximation

A master curve, summarizing the measured temperature histories at bottle center, was derived on the basis of Eq. 3. For each experimental condition, the characteristic time was calculated as $\tau = \frac{mc_p}{U_g A_s}$. The resulting curves are

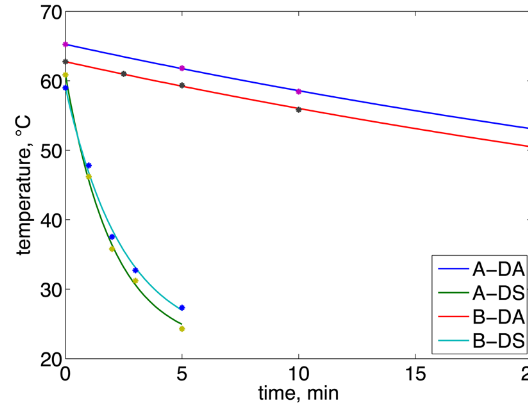

Fig. 7 Measured temperature at bottle center in dynamic tests and related fitting curve. *Each curve* is identified by three letters: X–YZ. *X* indicates the sample (A or B). Y = D is for dynamic bottle condition. Z stays for cooling media: *A* is air, *S* is spray

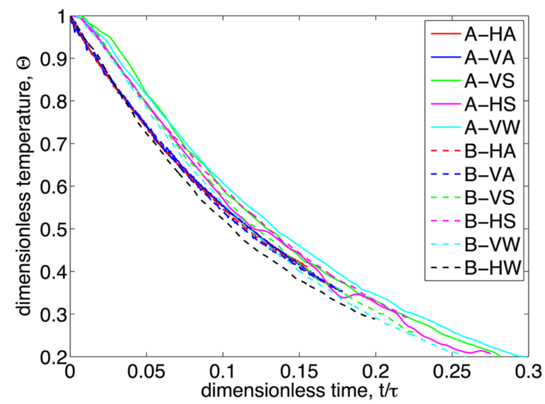

Fig. 8 Dimensionless temperature at the bottle center reported as a function of dimensionless time (Eq. 3). *Each curve* is identified by three letters: X–YZ. *X* indicates the sample (A or B). *Y* indicates the bottle position (*H* horizontal and *V* vertical). Z stays for cooling media: *A* is air, *S* is spray, *W* is water

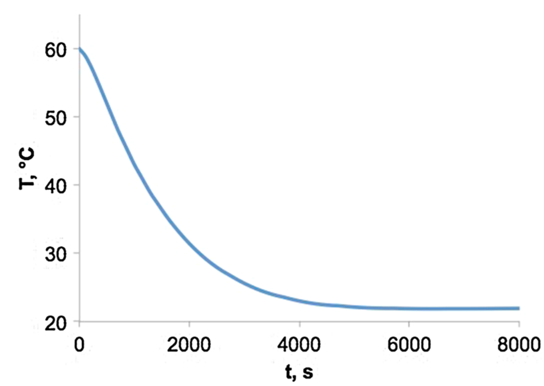

Fig. 9 Temperature at bottle center simulated via COMSOL multiphysics, assuming conductive heat transfer inside the bottle and an external heat transfer coefficient of 1000 W/m^2 K

Table 2 Summary of measured global heat transfer coefficients

Bottle motion	Cooling position	Cooling media	U_g Bottle A (W/m^{2}K)	U_g Bottle B (W/m^{2}K)	Difference $\frac{(A-B)}{A}$ (%)	Difference reason
Static	Vertical	Air	8.9 ± 0.9	9.0 ± 0.1	−1	–
		Water	136 ± 7.4	105 ± 5.7	23	L, C
		Spray	132 ± 11	129 ± 8.1	2	–
	Horizontal	Air	10.2 ± 0.5	10.6 ± 0.2	−4	–
		Water	170 ± 12	123 ± 16	27	L, C
		Spray	160 ± 5.5	147 ± 5.7	8	L
Dynamic	Horizontal	Air	15 ± 2.7	15 ± 1.7	0	–
		Spray	385 ± 24	317 ± 18	18	L

L PET layer, *C* internal convection

reported in Fig. 8: curves collapse on a narrow band, showing that a lumped system approximation is almost correct in all explored cases. Hence, even considering the internal transport as relevant in some of the cooling systems studied, temperature gaps can still be assumed as confined within a relatively narrow layer near the bottle surface, because the heat transfer is governed by convection instead of conduction. This justifies the lumped system assumption initially claimed.

4 Conclusions

Cooling of packed beverages is a critical step in many food industry applications and the understanding of transport phenomena, around and inside PET bottles, can provide a valid tool to decide whether or not those containers are suitable for low temperature pasteurization, or other thermal processes [17]. In order to calculate global heat transfer coefficient U_g, cooling tests were performed on two different PET bottle samples in different conditions. Results are summarized in Table 2. As expected, air cooling was extremely slow ($U_g \sim 10$ W/m^2 K) but increased 1.5 times in dynamic conditions. Water cooling was more than one order of magnitude faster and differences among water bath and spray were noticeable but not very significant (between 6 and 23 %). In agreement with literature, vertical position cooling was shown to be always slower than horizontal one. Dynamic cooling tests showed that rotation at 200 rpm enhanced heat transfer coefficient by 240 and 215 % for sample A and B respectively. As expected, PET wall thickness was shown to affect heat transfer coefficient increasingly with U_g value (differences among sample A and B ranging from 0 when U_g equal 10 W/m^2 K up to 20 % when U_g was nearly 400 W/m^2 K). Furthermore, it is remarkable that in static water cooling, a different heat transfer through the PET layer led to a different fluid dynamics condition for both inside and outside the bottle (see Fig. 5). When bottle was set in rotation, so when system was ruled by forced convection, this phenomenon lost importance. All things considered, the best condition is the dynamic cooling under water spray, which allows a cooling with characteristic time τ of about 150 s, compatible with typical cooling times after pasteurization processes. As the heat transfer is mainly limited by internal heat transfer coefficient, to further reduce the cooling time, different ways to promote internal mixing (e.g. shaking, rotation around different axes) should be explored.

Acknowledgments This research is part of the DIT (Dynamic Irreversible Thermoporation) project supported by PO FESR 2007/2013 fund of European Union.

Compliance with ethical standards

Conflict of interest The authors declare that they have no conflict of interest.

Appendix

Internal heat transfer coefficient

The theoretical case of pure diffusive heat transfer inside the bottle was considered.

Although this condition is not expected to be realistic for our case studies, its analysis is still very useful for data interpretation. Indeed, it allows one to define a limit heat transfer coefficient: any experimentally found U_g, if higher than the one calculated for pure diffusive heat transfer, would imply natural convection is occurring within the bottle. External heat transfer was considered extremely fast and PET wall was lumped with internal distilled water. This latter approximation is legit as thermal diffusivity of PET and water are very close ($\alpha_w = 1.43 \times 10^{-7}$ and $\alpha_{PET} = 1.5 \times 10^{-7}$) [18]. However, if those thermal diffusivities were not similar, by means of dimensional analysis the PET layer could be substituted with a fictitious water layer [19], thus solving a single diffusion equation instead than two distinct differential equations. In the case of pure conduction, the heat equation written in cylindrical coordinates is [13]:

$$\frac{\partial T}{\partial t} = \alpha * \frac{1}{r}\frac{\partial}{\partial r}\left(r\frac{\partial T}{\partial r}\right) \tag{9}$$

which must be solved with the following boundary conditions: at t = 0, $T = T_0$; at r = 0, $\partial T/\partial r = 0$; at $r = r_1 \approx r_2$, the conductive heat flux must be equal to the external convective heat flux. The characteristic time for this system, defining the shape of the T versus t curve, can be estimated as $\tau = R^2/\alpha$ [13]. When using the aforementioned values, calculated τ is around 7600 s. According to theory, after a time close to τ, equilibrium is achieved [20].

A simulation with COMSOL Multiphysics package, assuming pure heat conduction, gave nearly the same results (Fig. 9). The external heat transfer coefficient was set to 1000 W/m^2 K, to highlight the internal resistance.

In this way, the maximum cooling time was estimated, related to the worst heat transfer conditions inside the bottle. A lumped system with the same τ, would be characterized by a U_g in the order of 10^{-2} W/m^2 K, therefore any bigger U_g experimentally measured, would reasonably imply the presence of convection phenomena inside the bottle. Typical values for heat transfer coefficient of liquids in natural convection conditions are in the range 10–100 W/m^2 K [13]. Collected data always led to U_g in this order of magnitude, thus confirming the presence of natural convection phenomena inside the bottle.

External heat transfer coefficient

To get an estimate of external heat transfer coefficients during static cooling in air and water, different empirical correlations were employed. Nusselt number ($Nu = \frac{hD}{k}$, where D is the cylinder diameter) around horizontal cylinders can be calculated by means of empirical correlations Eq. 10 and 11 [21, 22].

$$Nu = \left\{0.6 + \frac{0.387Ra^{1/6}}{\left[1 + (0.559/Pr)^{9/16}\right]^{8/27}}\right\}^2 \tag{10}$$

$$Nu = C(\mathrm{Pr}) * Ra^{0.25} \tag{11}$$

In Eq. 11, C is a constant depending on Prandtl number value ($Pr = \frac{\mu c_p}{k}$, where μ is the fluid viscosity), which is 0.436 for air and 0.52 for water at ambient conditions. Rayleigh number is defined as Ra = Gr*Pr, with Gr being the Grashof number ($Gr = \frac{g\beta(T_{wall} - T_\infty)D^3}{\nu^2}$, where g is the gravitational acceleration, β the volumetric thermal expansion coefficient, ν the kinematic viscosity, T_{wall} the temperature at bottle surface and T_∞ the bulk temperature of cooling fluid).

In order to estimate Nu value in the case of vertically positioned bottle, Eq. 12 was used, which is suitable for vertical surfaces [21] and Eq. 13, for vertical cylinders [22].

$$Nu = \left\{0.825 + \frac{0.387Ra^{1/6}}{\left[1 + (0.492/Pr)^{9/16}\right]^{8/27}}\right\}^2 \tag{12}$$

$$Nu = \frac{4}{3}\left[7Gr\frac{Pr^2}{5(20 + 21Pr)}\right]^{0.25} + \frac{4H(272 + 315Pr)}{35D(64 + 63Pr)} \tag{13}$$

Results are summarized in Table 1, Theory and Methodology. Calculations for water led to h_2 two orders of magnitude higher than in the case of air.

Calculations worked out in order to estimate heat transfer coefficient in air dynamic cooling were based on the work by [23] on heat transfer from a heated rotating cylinder in still air. During rotation at 200 rpm, Reynolds number around bottle is about 2500, while Gr number is nearly 100,000. In this condition, the system cannot be considered as ruled by forced convection neither by natural convection only, and both Re and Gr numbers are needed in order to estimate Nusselt number. For the considered case, Nu is about 40, thus resulting in a heat transfer coefficient h_2 of about 17 W/m^2 K.

Heat transfer across PET layer

The scenario herein presented highlights how much PET layer thickness affects global heat transfer coefficient. Writing Eq. 3 as:

$$\theta = e^{\left(-\frac{U_g A}{m c_p}t\right)} \tag{14}$$

where θ is $(T-T_c)/(T_0-T_c)$, the time required to reach a certain dimensionless temperature θ can be calculated as:

$$t = -\frac{mc_p}{U_g A}\ln\theta \tag{15}$$

By substituting Eq. 1, Eq. 6 was derived:

$$t = -\frac{mc_p}{A}\left(\frac{1}{h_1} + \frac{1}{h_2} + \frac{\delta}{k}\right)\ln\theta \tag{16}$$

it can be noticed how cooling time is dependent on PET thickness δ. At high fluid dynamics regimes, where $1/h_1$ and $1/h_2$ are much smaller than δ/k, this effect becomes more important, and t is significantly influenced by δ [18].

References

1. Bischof JC, He X (2006) Thermal stability of proteins. Ann NY Acad Sci 1066:12–33

2. Hanschen FS et al (2012) Thermally induced degradation of aliphatic glucosinolates: identification of intermediary breakdown products and proposed degradation pathways. J Agric Food Chem 60(39):9890–9899
3. Jiménez-Sánchez C et al (2015) Alternatives to conventional thermal treatments in fruit-juice processing. Part 2: effect on composition, phytochemical content, and physicochemical, rheological, and organoleptic properties of fruit juices. Crit Rev Food Sci Nutr, p. posted online. ISSN:10.1080/10408398.2014.914019
4. Perussello CA, Viviana CM, Alvaro CDA (2011) Combined modeling of thermal properties and freezing process by convection applied to green beans. Appl Therm Eng 31:2894–2901
5. Berto MI, Silveira VJ (2013) Design and performance of conventional and fuzzy controls for a high temperature short time pasteurization system. J Food Process Eng 36:58–65
6. Bates RP, Morris JR, Crandall PG (2001) Principle and practice of small-and medium-scale fruit juice processing. FAO Agricultural Services Bulletin, Rome
7. Cammalleri M et al (2015) Experimental evaluation of a new thermal process for microorganisms inactivation. J Food Process Eng. doi:10.1111/jfpe.12175
8. Bach C et al (2013) Effect of temperature on the release of intentionally and non-intentionally added substances for poly-ethylene-terephtalate (PET) into water: chemical analysis and potential toxicity. Food Chem 139:672–680
9. Omari KE, Kouskou T, Guer YL (2011) Impact of shape of container on natural convection and melting inside enclosures used for passive cooling of electronic devices. Appl Therm Eng 31:3022–3035
10. Augusto PED, Pinheiro TF, Cristianini M (2012) Determining convective heat transfer coefficient (h) for heating and cooling of bottles in water immersion. J Food Process Eng 35:54–75
11. Haeri S, Shrimpton JS (2013) A correlation for the calculation of the local Nusselt number around circular cylinders in the range $10 \leq Re \leq 250$ and $0.1 \leq Pr \leq 40$. Int J Heat Mass Transf 59:219–229
12. Abu-Hijleh BA (2001) Laminar forced convection heat transfer from a cylinder covered with an orthotropic porous layer in cross-flow. J Numer Methods Heat Fluid Flow 11(2):106–120
13. Bird RB, Stewart WE, Lightfoot EN (2002) Transport phenomena, 2nd edn. Wiley, New York
14. Bernier D, Hansen GA (1972) Thermal conductivity of polyethylene: the effects of crystal size, density and orientation on the thermal conductivity. Polym Eng Sci 12:204–208
15. Choy CL, Chen FC, Luk WH (1980) Thermal conductivity of oriented crystalline polymers. J Polym Sci Polym Phys 18:1187–1207
16. Merk HJ, Prins JA (1954) Thermal Convection in Laminar Boundary Layers III. Appl Sci Res Sect A 4:207–221
17. Shanthi V, Agarwal P, Sikand A (2014) Application of heat exchangers in bioprocess industry: a review. Int J Pharm Pharm Sci 6:24–28
18. Morikawa J, Hashimoto T (1997) Study on thermal diffusivity of poly(ethylene terephthalate) and poly(ethylene naphthalate). Polymer 38:5397–5400
19. Mannella GA, la Carrubba V, Brucato V (2014) Peltier cells as temperature control elements: experimental characterization and modeling. Appl Therm Eng 63:234–245
20. Isachenko VP, Osipova VA, Sukomel AS (1987) Heat transfer. MIR, Moscow
21. Churchill S, Chu H (1975) Correlating equations for laminar and turbulent free convection from a vertical plate. Int J Heat Mass Transf 18:1323–1329
22. Bejan A, Kraus AD (2003) Heat transfer handbook. Wiley, Hoboken
23. Elghnam RI (2014) Experimental and numerical investigation of heat transfer from a heated horizontal cylinder rotating in still air around its axis. Ain Shams Eng J 5:177–185